

Removal of chromium and cadmium ions from aqueous solution using residue of *Rumex dentatus* L. plant waste

N.K. Soliman^{a,*}, Hussein S. Mohamed^{a,b}, Rasha H. Elsayed^b, Nashwa M. Elmedny^b, Ahmed H. Elghandour^b, Sayed A. Ahmed^b

^aBasic Science Department, Nahda University, Beni-Suef, Egypt, emails: nofal.khamis@nub.edu.eg (N.K. Soliman), h_gendy_2010@yahoo.com (H.S. Mohamed)

^bChemistry Department, Faculty of Science, Beni-Suef University, Beni-Suef, Egypt, emails: Rasha.sci8@gmail.com (R.H. Elsayed), rabahelpop@gmail.com (N.M. Elmedny), elghandourchem4ever@yahoo.com (A.H. Elghandour), Skader_70@yahoo.com (S.A. Ahmed)

Received 5 August 2018; Accepted 24 January 2019

ABSTRACT

In this work, residue powder of brown *Rumex dentatus* L. plant (*R*), after extracting most of its active components by 70% ethanol is used as an adsorbent for wastewater treatment. The biosorbent *R* before and after adsorption processes was investigated using Fourier-transform infrared spectroscopy and scanning electron microscopy. The factors affecting adsorption of Cd^{2+} and Cr^{3+} onto *R* such as biomass weight, initial concentration, contact time, temperature and pH were studied and the results showed that *R* had higher metal uptake percentage reaching 98.6% and 98.1 for Cd^{2+} and Cr^{3+} , respectively, at pH, 50 mg of catalyst, 25°C and initial metal concentration of 100 mg L⁻¹. The adsorption isotherm showed that Cd^{2+} adsorption follows Freundlich isotherms while Cr^{3+} fitted with Temkin isotherm and pseudo-second-order kinetics for both metal ions and the maximum amounts of metal ions adsorbed were found to be 81.76 and 31.5 mg g⁻¹ for Cd^{2+} and Cr^{3+} , respectively. Reusability test of *R* showed that *R* was effectively reusable adsorbent for both metal ions.

Keywords: Plant residue; *Rumex dentatus* L. plant; Adsorption; Toxic heavy metals; Isotherms; Kinetics

1. Introduction

Through the last few decades, the industrial progress and growing population have participated in an increase in ecosystems pollution, particularly aquatic environment, by heavy metals [1]. Water pollution is a very dangerous problem which causes many diseases since it is found that 2 million deaths and 4 billion diarrhea cases result from water pollution [2].

Heavy metals are very hurtful pollutants for all living organisms because they are toxic, stable and non-biodegradable. They also tend to accumulate in the food chain of the organisms, which leads to many diseases and functional disorders. In various industrial wastewaters,

cadmium and chromium are present and they are very toxic metals and cause many environmental problems. Cadmium is an environmental pollutant which is produced from the fuel combustion, metallurgy, metal plating, cement, ceramic production, pigments, and batteries industries. Even low concentration of cadmium (II) in water causes very harmful diseases such as chronic lung disorders, kidney deterioration, proteinuria, skeletal distortion, and testicular atrophy and even muscular cramps [3,4]. Chromium is a very common water pollutant which could be found in several states (solid, liquid, and gas states). Among several oxidation states of chromium, Cr^{+3} and Cr^{+6} are the most abundant states of chromium. Both forms are toxic in high dosages for all living organisms but Cr(IV) is the most harmful and has higher water solubility than Cr(III) . Usually, Cr(III) is oxidized into

* Corresponding author.

Cr(IV) due to a large amount of oxygen in the environment. So, we must get rid of any chromium pollution.

Cr(III) is selected instead of Cr(VI) in our study because of following reasons, Cr(III) is toxic if excess quantity is taken and causes abnormalities in organisms where Cr(III) compounds affect the respiratory tract and cause an increase in lung weight. Also they have an immunological effect. Cr(III) also has a negative effect on reproduction process [5,6]. Several industries are based on using chromium such as the manufacture of paints and paper, mining and electroplating. All of these industries participate in producing water pollution with chromium when introduced into the environment through sewage [7]. World Health Organization WHO (2008), determined the maximum admissible limit of cadmium and chromium in drinking water to be 3 and 50 $\mu\text{g L}^{-1}$, respectively [8].

Many techniques are used for solving water pollution problems such as solvent extraction, chemical precipitation, flocculation, reverse osmosis, membrane filtration, ion exchange, cementation, and adsorption [9]. The adsorption is one of the most effective techniques which are used in this field due to its high applicability and low cost [10]. Moreover, adsorption has advantages over the other wastewater treatment techniques because it has a simple design with a sludge-free environment and can involve low investment in terms of both initial cost and land required [11].

The researchers introduced many adsorbents for heavy metal removal such as the activated carbon which is widely used as an effective adsorbent but it is very expensive to be used in wastewater treatment. Also, the agriculture wastes are used as adsorbents such as rice husk, coconut husk, wheat bran and the activated carbon derived from them which are low-cost adsorbents. However, their use is limited because it is difficult to get rid of them after adsorption process [12]. Some modified naturally occurring materials are also used such as modified chitosan composites [13], zeolites and clay minerals [14]. Nanostructured materials such as carbon nanotubes and fullerenes are used in adsorption process [14].

The use of waste materials as low-cost adsorbents is attractive due to their contribution to the reduction of costs for waste disposal [15].

Rumex dentatus L. is a wild edible plant growing in many countries where *R. dentatus* is considered one of the most abundant *Rumex* species present in Egypt. *R. dentatus* belongs to the family of Polygonaceae and it is known as dentate dock which is used as a medical plant because it has anti-bacterial, anti-inflammatory, anti-tumor, anti-dermatitis, and antioxidant properties. *R. dentatus* is known to be rich with anthraquinones and chromones [16].

R. dentatus includes a variety of compounds that are biologically active since its leaves contain a large amount of oxalic acid (0.3%) and tannins (7%–15%) where it was found that the large content of tannins in leaves was responsible for phytoremediation of lead through chelation of lead by tannins. It also contains a high level of polyphenolic compounds which have a good effect on metal accumulation. The extract of this plant was used to increase phytoremediation of *Plantago major* L. in soil contaminated by carbosulfan [17].

In this study, we use the residues of *R. dentatus* plant, *R*, after the extraction of phytochemicals from it to study

its ability for heavy metal removal. This is the first time the *R. dentatus* wastes have been used as an adsorbent for heavy metals. *R* was chosen for the following reasons: (1) it is a cheap and abundant adsorbent as the cost and abundance of the adsorbent are an important factor that must be considered when selecting an adsorbent. (2) The low-cost of regeneration and reuse of *R*. The regeneration and reuse of *R* may play an important role in making this a practical process. Also the cost of regeneration/disposal of the spent adsorbent would have to be considered in any detailed economic analysis required to determine the most economical adsorbent.

Also, in this paper we studied the factors that affect the adsorption process such as biomass weight, the initial concentration of metal ions, time, temperature, and pH. Adsorption isotherm, kinetics, and re-usability of *R* were also studied.

2. Materials and methods

2.1. Adsorbent preparation

The Aerial parts of *Rumex dentatus* L. were collected and identified at Botany department in Beni-Suef University.

The aerial parts of *R. dentatus* were washed with tap water and distilled water numerous times to remove the unwanted materials and dried under shake at room temperature. The air-dried plant was grinded by blender into powder to increase the surface area then it was soaked in ethanol 70% for several days to make phytochemicals extraction. The residual parts of *R. dentatus*, (called *R*) after the completion of the extraction process were well dried and used in the heavy metal removal process.

The residual plant biomass is identified before and after metal ions adsorption process using Fourier-transform infrared spectroscopy (FTIR) (Tensor – 27. Bruker FTIR model), with the wave number 500–5,000 cm^{-1} under normal conditions, and scanning electron microscopy (SEM) (a JEOL, JSM-52500 LV SEM, Japan).

2.2. Adsorption experiments

Cd^{2+} and Cr^{3+} metal ions were selected for studying of adsorption process. Cd^{2+} and Cr^{3+} ions solutions with concentrations (10, 25, 50, and 100 mg L^{-1}) were prepared by dissolving the salts of $\text{CrCl}_3 \cdot 6\text{H}_2\text{O}$ and $\text{CdCl}_2 \cdot \text{H}_2\text{O}$, respectively, in distilled water and then mixed with alga waste (*R*). Measurements of the adsorption behavior, isotherm and kinetics at different reaction conditions including initial metals ions concentration, concentrations of adsorbent (waste of alga), pH of the metals ions solution were done as follows, at specific time interval the changes in the concentration of the tested metals ions were measured using atomic absorption spectrometer (PerkinElmer A Analyst 100, USA).

2.2.1. Effect of the initial metal ions concentration

Studying the effect of initial metal ions concentrations was done at constant kinetic parameters, temperature (room temperature 25°C), pH = 6.2, and catalysts weight (50 mg). The adsorption kinetic experiments were carried out by adding 50 mg of *R* to 100 mL of the tested metal solutions

of different concentrations (10, 25, 50, and 100 mg L⁻¹) with shaking. Each concentration sample was measured at fixed time intervals (30, 60, 90, 120, and 180 min).

2.2.2. Effect of the catalyst weight

At pH 6.2 and 25°C, different amounts of adsorbent (10, 30, 50, and 70 mg) were added and shaken with 100 mL solution of 100 mg metal L⁻¹ concentration and 180 min contact time.

2.2.3. Effect of operating temperature

The operating temperature effect was studied at different temperatures (25°C, 40°C, 60°C, and 80°C) and constant kinetic parameters of catalyst weight (50 mg), metals ions concentration (100 mg L⁻¹) and pH degree = 6.2 and 180 min contact time. After each run, the solid was collected after filtration and washed several times by distilled water to be used in the second run.

2.2.4. pH effect

The influence of pH value was studied at pH = 3, 5, 6.2, and 8 on the adsorption process at constant temperature (25°C), catalyst weight (50 mg) and initial metals ions concentration (100 mg L⁻¹) and 180 min contact time.

2.2.5. Reusability of R

For examination of the reusability of the R, the adsorption process was carried out four times with the same adsorbent using 50 mg of the catalyst at pH = 6.2 and constant temperature (25°C) and 180 min contact time for each cycle.

2.3. Statistical analysis

The adsorption data were a mean of three independent experiments. The regression coefficient (R^2) values of Langmuir, Freundlich, Temkin isotherm, pseudo-first-order, pseudo-second-order, intraparticle diffusion, and Elovich kinetic models were determined by using statistical functions of Microsoft Excel 2007 version.

The amount of metals ions adsorbed onto (R) at equilibrium q_e (mg g⁻¹), the amount of metals ions adsorbed onto R at any time q_t , and the metals ions removal % were calculated according to Eqs. (1)–(3), respectively [18,19].

$$q_e = \frac{V(C_0 - C_e)}{m} \quad (1)$$

$$q_t = \frac{V(C_0 - C_t)}{m} \quad (2)$$

$$\text{metal ion removal \%} = \frac{(C_0 - C_t)}{C_0} \times 100 \quad (3)$$

where C_0 , C_t and C_e are the metals ions concentrations (mg L⁻¹) in; the initial solution, the solution after time t and the solution at equilibration, respectively. While V is the solution volume in mL and m is the adsorbent mass in mg.

3. Results and discussion

3.1. Characterization of R

3.1.1. Fourier transformer infrared analysis

FTIR examination was done to determine the type of interaction between the adsorbent and the adsorbed metals. As shown in Fig. 1, the spectrum of *R. dentatus* waste before and after adsorption basically was unchanged but we noted that there was a slight shift in the frequency of some peaks and also changes in the peaks intensity which indicated that the adsorption process occurred without damage of plant surface [20]. Strong absorption at 3,470 and 3,290 cm⁻¹ was observed before and after metals adsorption which attributed to the presence of OH and –NH groups which were compatible with C–O and C–N bands at 1,050 and 1,110 cm⁻¹, respectively [21]. The peaks at 3,150 and 2,880 cm⁻¹ are related to C–H stretching band in aliphatic and aromatic form. These bands elucidated with the peaks which appeared at 1,660 and 1,590 cm⁻¹ related to C=C stretching band and 1,430 cm⁻¹ related to C–H bending [22]. The peak at 1,550 cm⁻¹ was related to the N–H bending band [23]. The decrease in absorbance intensity is observed after Cd²⁺ and Cr³⁺ adsorption in broad band which may be related to O–H carboxylic group which referred to the interaction of this group with metal ions. Also, the decrease in frequency value of C–H aromatic band after cadmium adsorption confirmed the adsorption process. Presence of ionizable functional groups such as OH, C=O and –NH would help in the removal of heavy metal ions due to their ability to interact with the positively charged metal ions [24].

3.1.2. SEM characterization

The SEM images of R before and after metal adsorption at 2,000 × magnification are shown in Fig. 2. The morphology of the adsorbents surface before and after extraction process and also after metal ion uptake was investigated using SEM analysis. Noticeable changes to the surface morphology

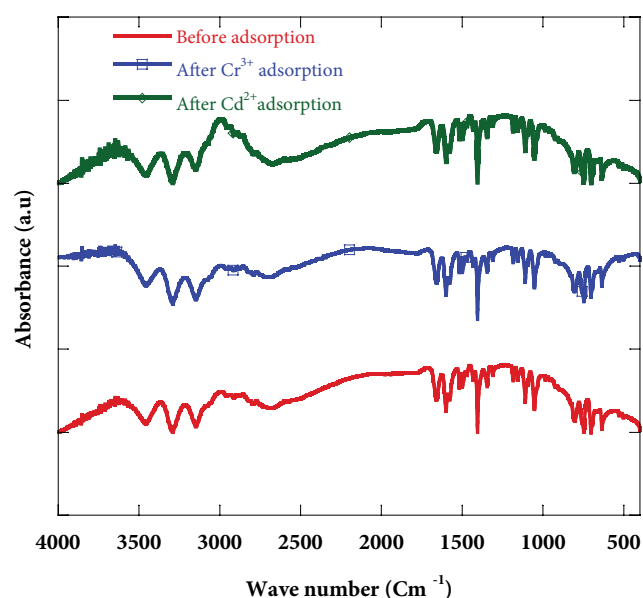


Fig. 1. FT-IR of R before and after adsorption processes.

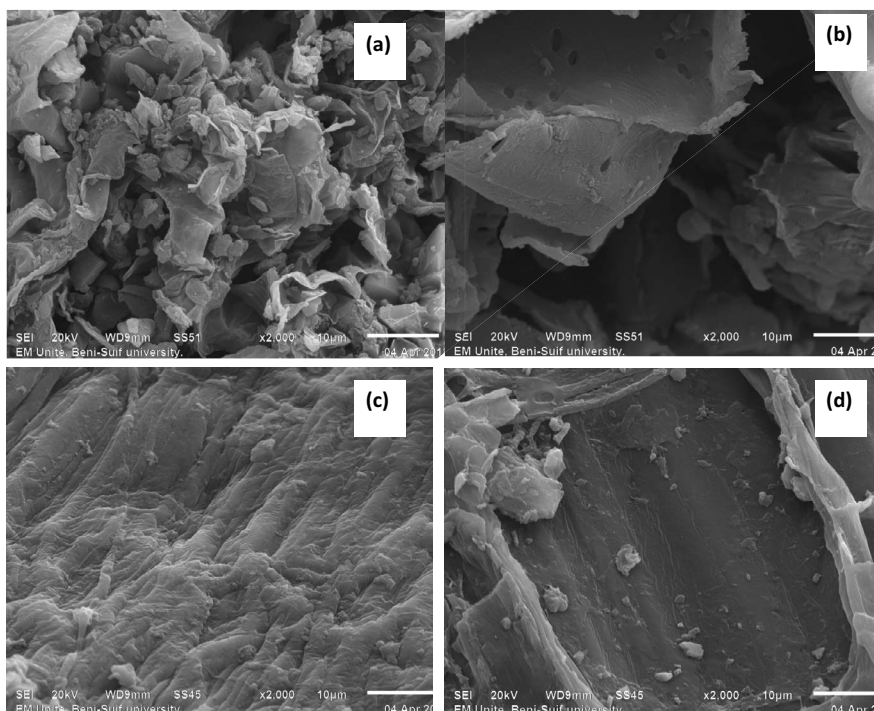


Fig. 2. SEM image of *R* where: (a) before soaking in 70% methanol, (b) after soaking in 70% methanol, (c) after Cd^{2+} adsorption and (d) after Cr^{3+} adsorption.

of the biosorbents were observed, the plant before the extraction process showed uneven surface with cracks and there were no visible pores but after the extraction the surface became smoother and porous and the surface was characterized by micro and macro pores and cavities as shown in Figs. 2(a) and (b). This change interprets the increase in metal uptake percentage of the extracted plant (waste) more than the untreated one where the ethanol extraction process liberates the compounds from plant surface and opens up the pores on cell wall [25]. After contact with cadmium and chromium ions solutions (Figs. 2(c) and (d)), the cells became swollen, damaged, with meanders surface and the holes were covered with the adsorbed metal ions particles. These resulted in changes perhaps because of the metals ions collected around the cells and associated with their functional groups as well, these changes may be produced during the exposure of the samples to heavy metal solutions; where solution metal ions replace some of the cations that initially found in the cell wall matrix. Because of the ion-exchange mechanism, the heavy metals fill the ready unoccupied binding sites [26].

3.2. Effect of initial metal ions concentration and contact time

Figs. 3 and 4 show the relationship between the initial metal ions concentrations with contact time and the percentage of metals removal and the amounts of adsorbed metals ions using (*R*) as an adsorbent. From Fig. 3, it was concluded that at the first stage, the adsorption rate was very high throughout the initial 30 min. Then it was decreased till it reached the equilibrium state. The rate of adsorption at the first stage of the adsorption process is rapid. This may be

attributed to a large number of empty adsorption sites existing on the adsorbent surface. With time, these vacant sites become occupied by the adsorbed metal ions that produce a repulsive force between the molecules of adsorbate metal ions on *R* surface and in bulk liquid phase as obtained from Figs. 3 and 4 [27,28] and consequently the adsorption rate decreases as shown in Figs. 3, 4(a), and 4(b).

For the two tested metals ions, the *R* catalyst causes heavy metal removal percentage of 90.3%, 85.3%, 84.3%, and 81.7% after approximately 180 min for Cd^{2+} metal ions solution with concentrations of 10, 25, 50, and 100 mg L^{-1} , respectively, and remove 62.6%, 88.7%, 85.8%, and 84.2% after approximately 180 min for Cr^{3+} metal ions solution with concentrations 10, 25, 50, and 100 mg L^{-1} respectively. This activity may be due to the synergetic effect of the active components of *R*. The two metal ions Cd^{2+} and Cr^{3+} show the same behavior where the metal ions removal % is higher with lower initial metal ions concentration except for Cr^{3+} metal ion with initial concentration 10 mg L^{-1} . It shows a lower removal %. This phenomenon may be attributed to increasing concentration gradient with increasing metal ions initial concentration. Consequently, the driving force, which has the capability to overcome the resistance of mass transfer between the liquid and solid phases, will be increased [29].

From Figs. 4(a) and (b), an increase in the amounts of adsorbed metal ions is observed with the increase in the concentration of initial metal ions. This phenomenon may be because of the excess in the driving force of the concentration gradient with the higher initial metal concentration which has the capability to overcome the strength of mass transfer between the solid and liquid phases [29].

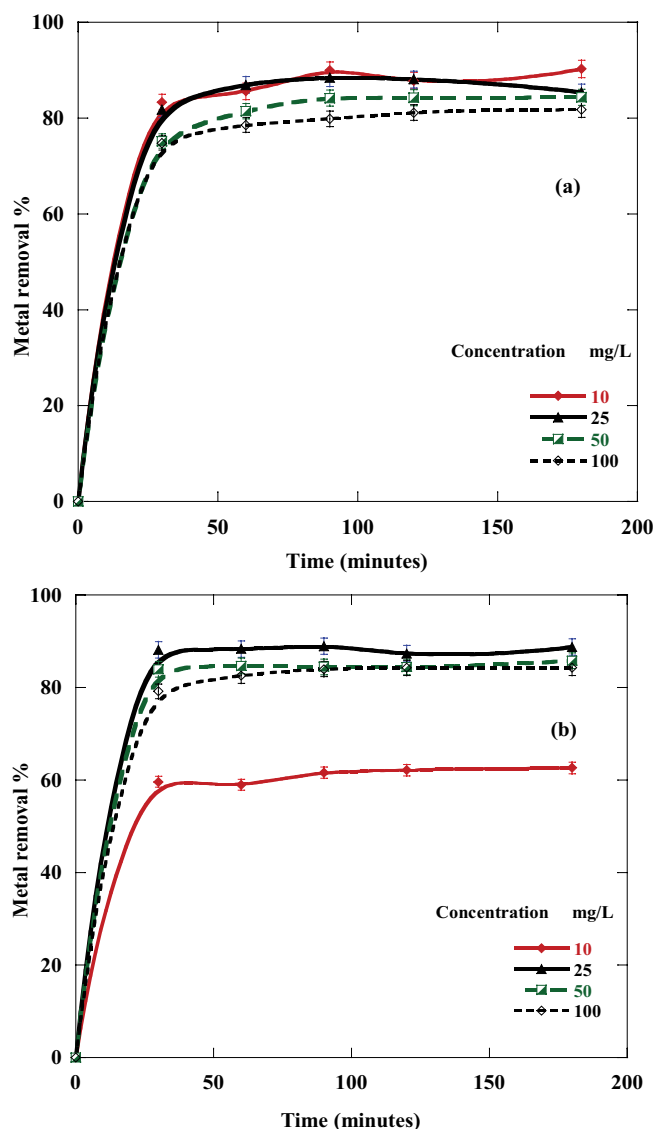


Fig. 3. Effect of metal concentration and contact time on the removal % of metal ion adsorbed by 50 mg of R at 25°C and pH 6.2. (a) Cd²⁺ and (b) Cr³⁺.

The maximum amounts of metals ions adsorbed were found to be 81.76 and 31.5 mg g⁻¹ for Cd²⁺ and Cr³⁺, respectively, at 100 mg L⁻¹ concentration, temperature of 25°C and pH value of 6.2.

3.3. Adsorption isotherm

Adsorption isotherms are used to make us understand how the metal ions diffuse between adsorbent solid and solvent liquid phases. Adsorption isotherm equations are characterized by constant values that provide information about the affinity and the surface properties of the catalyst. They can be used to compare the adsorptive capacities of the R toward different pollutants.

Some of the normally known adsorption models are used to analyze the equilibrium data. The obtained experimental data of adsorption isotherms can be analyzed by using

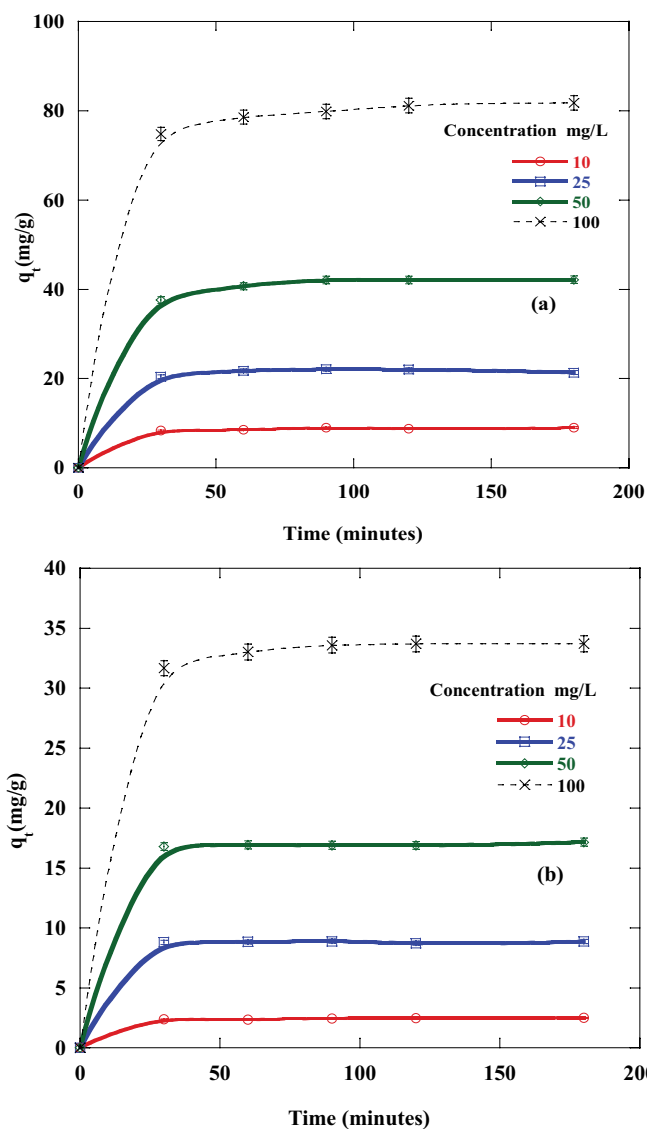


Fig. 4. Effect of metal concentration and contact time on the amount of metal ion adsorbed by 50 mg of R at 25°C and pH 6.2. (a) Cd²⁺ and (b) Cr³⁺.

several mathematical models. In this paper, three adsorption isotherms namely Langmuir, Freundlich, and Temkin were used to describe the adsorption isotherm for the investigated metal ions.

The Langmuir isotherm supposes that adsorption happens at active sites on the catalyst with monolayer adsorption and there is no interaction between the adsorbed metals ions. The Langmuir isotherm equation is expressed by Eq. (4) [30]:

$$\frac{C_e}{q_e} = \frac{1}{K_L Q_0} + \frac{C_e}{Q_0} \quad (4)$$

where q_e is the quantity of adsorbed metals ions at equilibrium time (mg g⁻¹), Q_0 is the maximum quantity of adsorbed metals ions on R adsorbent catalyst (mg g⁻¹), C_e is

the concentration of the tested metal ions at equilibrium (mg L^{-1}), and K_L is the Langmuir constant (L mg^{-1}).

The Freundlich model postulates that multilayer adsorption occurs on the adsorbent surface and there are unequal available heterogeneous sites with extraordinary energies of adsorption. The model also assumes that there is an interaction between adsorbed metal ions molecules. The Freundlich isotherm can be written as follows [31]:

$$\log q_e = \log K_F + \frac{1}{n} \log C_e \quad (5)$$

where K_F is the adsorbent capacity for Freundlich and n is the Freundlich adsorption intensity constant.

In the Temkin isotherm, the adsorption heat is reduced linearly with coverage. In addition, the adsorption process is distinguished by a regular distribution of binding energies, up to some maximum binding energy [32,33]. The Temkin isotherm equation can be written as follows:

$$q_e = B \ln K_T + B \ln C_e \quad (6)$$

where B is constant $B = (RT/b)$ and is related to the heat of adsorption and K_T is the Temkin's constant measured in (L mol^{-1}) which corresponds to the maximum binding energy. In addition, the absolute temperature (T) measured in (K) and the constant R which corresponds to the universal gas constant = $8.314 \text{ J mol}^{-1} \text{ K}^{-1}$.

Examination of the applicability of the three isotherms models for the adsorption process of Cd^{2+} and Cr^{3+} at different initial concentrations requires drawing linear plots of C_e/q_e against C_e , $\log q_e$ against $\log C_e$, and q_e against $\ln C_e$. The linear plots of Langmuir, Freundlich, and Temkin isotherms for the tested metal ions are shown in Figs. 5(a)–(c), respectively. The evaluated model parameters and correlation coefficient (the values of Q_m , K_L , K_F , and $1/n$, K_T , B , and R^2) for the three isotherms are given in Table 1. The values of R^2 (correlation coefficient) are considered as a measure of the validity and applicability of the experimental data suitability to the isotherm models.

From the data in Table 1, we can deduce that Temkin and Langmuir isotherms are invalid isotherms of Cd^{2+} adsorption onto adsorbent R . The value of R^2 is the greatest in case of Freundlich isotherm for Cd^{2+} metal ions and this refers to an increase in the probability that the adsorption process follows Freundlich models. Hence multilayer adsorption of metal ions occurs at the active sites on the catalyst which are unequal available heterogeneous sites, with different adsorption energies and with interaction between adsorbed molecules.

In the adsorption process of Cd^{2+} on R , the values of $(1/n)$ in the Freundlich isotherm model are less than unity. This refers to the adsorption process is favored and the surface is heterogeneous with lower interactions between the adsorbed ions and implies also that the adsorption of Cd^{2+} occurs by multi-molecular and multi-anchorage adsorption mechanisms, respectively [34,35].

For Cr^{3+} metal ions, the R^2 value is the largest in case of Temkin isotherm. This means that the adsorption process of Cr^{3+} approximately proceeds through Temkin isotherm models.

The correlation coefficient is 0.9988 for Freundlich isotherms with Cd^{2+} ions solution and 0.8716 for Temkin isotherm for Cr^{3+} ion adsorption at 25°C .

3.4. Adsorption kinetics

The adsorption kinetics of Cd^{2+} and Cr^{3+} onto R are analyzed by four adsorption kinetic models specifically the pseudo-first, second-order, intraparticle diffusion, and simple Elovich kinetic models in order to determine the adsorption mechanism and the rate determining steps of the adsorption process.

The pseudo-first-order rate equations are usually utilized to describe the adsorption kinetics of Cd^{2+} and Cr^{3+} metal ions from the aqueous solution can be described by Eq. (7) [36–38]:

$$\ln(q_e - q_t) = \ln q_e - k \times t \quad (7)$$

where q_e is the amount of the Cd^{2+} and Cr^{3+} (adsorbed molecules) onto R (adsorbent) at equilibrium time (mg g^{-1}), q_t is the amount of metals ions adsorbed on the catalyst at time t (mg g^{-1}), k is the first-order rate constant (min^{-1}). The adsorption rate in the pseudo-first order is directly proportional to the number of unoccupied sites on the adsorbent surface.

Pseudo-second-order model supposes that the adsorption rate is dependent on the square number of free active sites on the catalyst surface. The mathematical equation for pseudo-second-order kinetic model can be portrayed as given by Eq. (8) [39–41]:

$$\frac{t}{q_t} = \frac{1}{k_1 q_e^2} + \frac{t}{q_e} \quad (8)$$

where k_1 is the second-order rate constant.

Intraparticle diffusion kinetic models describe the movement of the metal ions dissolved in water from the liquid phase to the catalyst then the intraparticle diffusion process occurs [42]. Intraparticle diffusion equation can be written as follows:

$$q_t = k_2 t^{1/2} + I \quad (9)$$

where k_2 is the rate constant for intraparticle diffusion and I is the intercept that is relative to the boundary layer thickness.

Elovich kinetic model is considered as a special case of the second-order kinetics which indicates that adsorption process occurs chemically [43] if the catalyst surfaces are not energetically homogeneous [44]. The equation of Elovich model can be written as given by Eq. (10) [44]:

$$q_t = \frac{1}{\beta} \ln \alpha \beta + \frac{1}{\beta} \ln t \quad (10)$$

where α (mg min^{-1}) is the rate of initial adsorption at contact time $t = 0 \text{ min}$ and β (g mg^{-1}) is the extent of surface coverage and activated energy.

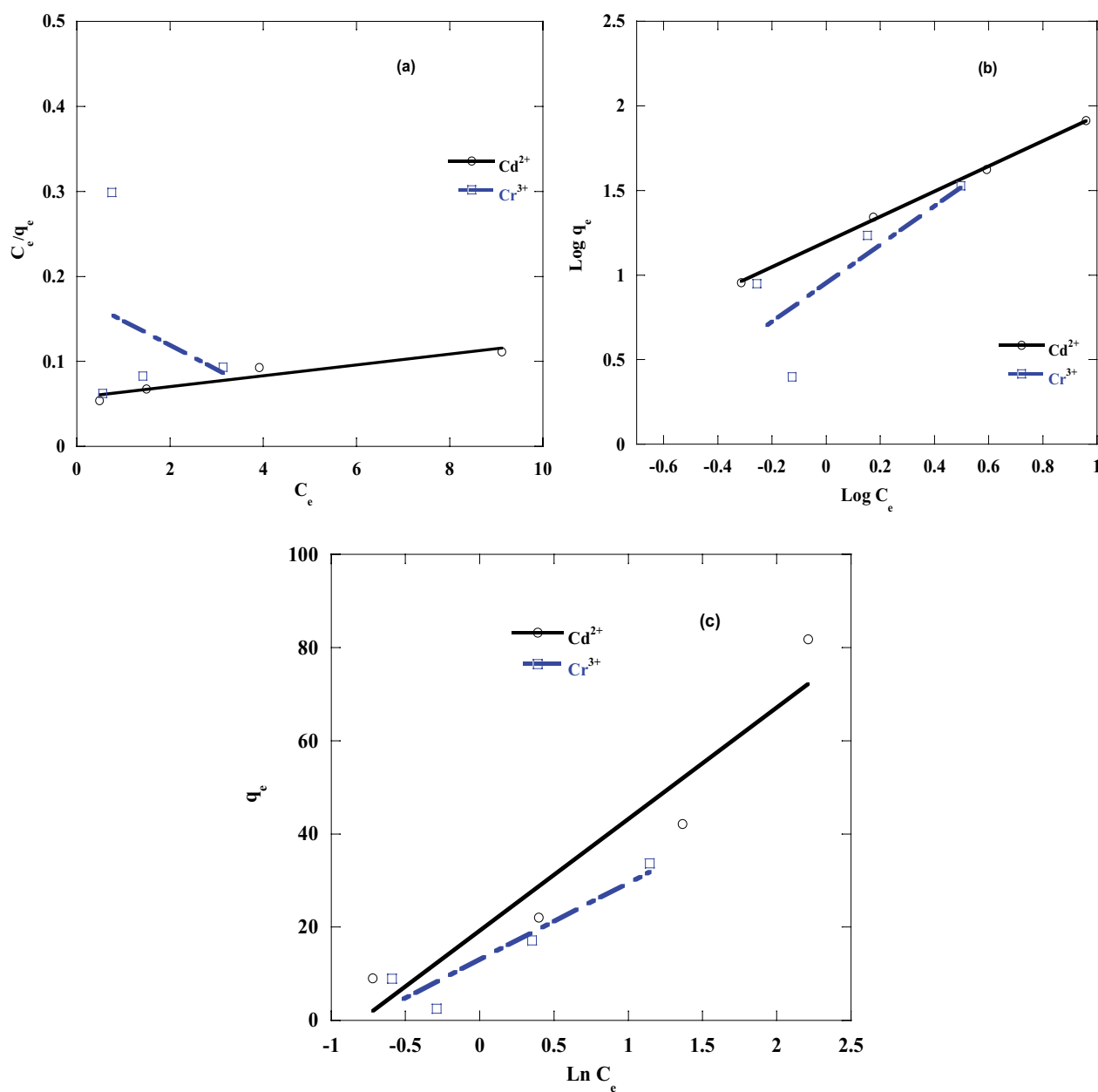


Fig. 5. Adsorption isotherm of Cd²⁺ and Cr³⁺ by 50 mg of R at 25°C and pH 6.2 where (a) Langmuir isotherms, (b) Freundlich isotherms, and (c) Temkin isotherms.

To study the applicability of the first order, second-order, intraparticle diffusion, and Elovich kinetic model for metal ions adsorption onto R from metal ion solution linear plots of $\ln(q_e - q_t)$ against t , t/q_t vs. t , q_t against $t^{1/2}$ and q_t vs. $\ln t$ must be plotted. The values of k , k_1 , k_2 , q_e , I , α , β , and R^2 are shown in Table 2.

The linear fit of all kinetic models and the values of R^2 for each graph are given in Table 2 which shows that the adsorption kinetics of the investigated metals ions onto R follows pseudo-second-order model that is consistent with the results of other works [45,46].

In addition, the experimental q_e ($q_{e,exp}$) values were compatible with the calculated ones (q_e), obtained from the linear plots of pseudo-second-order model shown in Fig. 6

and Table 2 at all investigated initial metal ions concentrations which indicate that the adsorption of Cd²⁺ and Cr³⁺ onto R follows pseudo-second-order kinetic model.

These indicated that the pseudo-second-order adsorption mechanism was prevailing and the overall rate of adsorption seemed to be a chemically controlled process involving valence forces through electrons sharing or exchange between adsorbed metals ions and the adsorbent R. The liquid-film diffusion (external diffusion) involves the movement of Cd²⁺ and Cr³⁺ molecules from the bulk of the solution towards the external surface of R. This step is followed by the adsorption of the R molecules on the surface of R adsorbent and chemically bonded to the surface of R. This was elucidated by the data obtained from FTIR which

shows the presence of functional groups which have the ability to make chemical bonds with heavy metals. Also it was found that; the pseudo-second-order rate constant (k) value is decreased with an increase in the initial concentration of the investigated metals ions. Similar kinetics also observed in the removal of Congo Red dye by cattail root [47], adsorption of malachite green on polylactide/spent brewery grains films [48] and adsorption of methylene blue on papaya seeds [49].

Table 1
Isotherm constants for Cd^{2+} and Cr^{3+} by 50 mg of R at 25°C and pH 6.2

Metal ions		Langmuir isotherm		
Constants	Q_0 (mg g ⁻¹)	K_L (L mg ⁻¹)	R^2	
Cd^{2+}	156.74	0.11	0.9131	
Cr^{3+}	-35.1	-0.16	0.093	
		Freundlich isotherm		
	$1/n$	K_F	R^2	
Cd^{2+}	0.744	15.7	0.9988	
Cr^{3+}	1.136	8.95	0.621	
		Temkin isotherm		
	B (J mol ⁻¹)	K_T (L mol ⁻¹)	R^2	
Cd^{2+}	23.93	2.24	0.9061	
Cr^{3+}	16.403	2.22	0.8716	

Table 2
Parameters of the kinetic models for Cd^{2+} and Cr^{3+} adsorption by 50 mg of R at 25°C and pH 6.2

First-order kinetic model								
Concentration (ppm)	Metal ions Cd^{2+}				Cr^{3+}			
	100	50	25	10	100	50	25	10
K	16.1×10^{-3}	26×10^{-3}	7.9×10^{-3}	15.5×10^{-3}	24.5×10^{-3}	12.4×10^{-3}	10.1×10^{-3}	15.8×10^{-3}
Q_e	5.1	4.71	1.82	1.76	3.74	1.74	1	1.05
R^2	0.9152	0.9152	0.9152	0.9152	0.9779	0.5408	0.5077	0.8554
$q_{e,\text{exp}}$	81.76	42.16	22.02	9.02	31.5	15.5	8.83	2.43
Second-order kinetic model								
K	2.7×10^{-3}	6.4×10^{-3}	96×10^{-3}	31.8×10^{-3}	14.8×10^{-3}	47×10^{-3}	339×10^{-3}	124×10^{-3}
q_e	90.9	43.5	21.7	9.17	34.1	17.2	8.86	2.54
R^2	0.9999	0.9996	0.9986	0.9994	0.9999	0.9998	0.9998	0.9997
$q_{e,\text{exp}}$	81.76	42.16	22.02	9.02	31.5	15.5	8.83	2.43
Intraparticle diffusion kinetic model								
K	5.9	3.08	1.56	0.65	2.43	1.21	0.627	0.179
I	19.6	9.87	5.66	2.19	8.5	4.58	2.443	0.6256
R^2	0.7337	0.6961	0.6967	0.7267	0.7139	0.6822	0.6701	0.7145
Elovich kinetic model								
β (g mg ⁻¹)	0.25	0.38	1.67	2.57	0.847	6.21	84.03	12.5
α (mg min ⁻¹)	1,590,729	28,190	10×10^{13}	17×10^7	2.2×10^{10}	7.6×10^{42}	1.3×10^{318}	1.5×10^{10}
R^2	0.9635	0.8443	0.3643	0.8161	0.8697	0.6336	0.0169	0.7378

3.5. Effect of catalyst weight

The quantity of catalyst used in metal removal is very important because it determines the equilibrium between the sorbent and sorbate and also predicts the cost of adsorption for each unit of aqueous solutions. The effect of catalyst weight on the removal % of Cd^{2+} and Cr^{3+} was investigated and the results are shown in Fig. 7. It can be deduced that the removal % of Cd^{2+} and Cr^{3+} increases as the catalyst weight increases from 10 to 50 mg and after that it decreases as illustrated from Fig. 7. This behavior may be due to the large surface area of the catalyst as the catalyst weight increases till it reaches 50 mg of catalyst [47]. On the other hand, by increasing the catalyst weight from 50 to 70 mg, the removal % decreases because the large adsorbent quantity cause cell agglomeration and consequently the intercellular distance decreases which creates 'screen effect' among a dense layer of cells leading to protection of the binding sites from metal ions [50]. The obtained data were in agreement with those of researchers who reported lower metal removal % at the high adsorbent weight [51,52].

3.6. Effect of pH

The adsorption capacity of metal ions is controlled by the initial pH of the aqueous solution where it affects the chemistry of the catalyst surface and also the ionization and dissociation of the sorbent molecule [53]. The effect of the initial solution's pH in the removal percentage of Cd^{2+} and Cr^{3+} onto R waste is shown in Fig. 8.

The relatively lower adsorption capacity for Cd^{2+} and Cr^{3+} in acidic conditions was attributed to the protonation

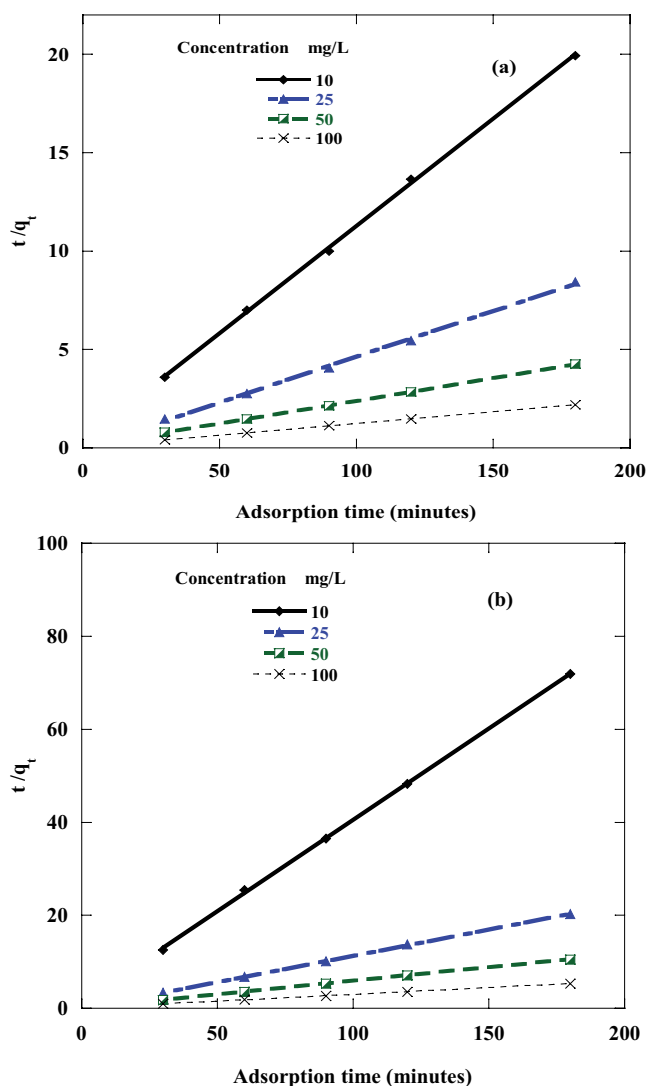


Fig. 6. Pseudo-second-order sorption kinetics of metal ions by 50 mg of R at 25°C and pH 6.2 (a) Cd²⁺ and (b) Cr³⁺.

of the catalyst surface as a result of the high concentration of H₃O⁺ ions which compete with metal ions throughout the adsorption process [54]. As the pH values increased to 5, the concentration of protons as competitors decreased consequently the metal ions uptake by the adsorbents increased reached to 96.1% and 96.6% for Cd²⁺ and Cr³⁺, respectively [55]. The increase in pH of the solution also led to a decrease in the number of positively charged available sites and an increase in the number of negatively charged active sites so the surface of adsorbent became negatively charged and the adsorption of positively charged metal (Cd²⁺ and Cr³⁺) ions by electrostatic forces of attraction and ion exchange were increased [56]. The last manner of increasing metal removal percentage as pH increase was followed till pH 5 then increasing pH to 6.2 was led to decrease in metal uptake not only due to the formation of soluble metal hydroxyl complexes (cadmium ions in form of Cd(OH)₂ and chromium ions in the form of Cr(OH)₃) but also to the ionized nature of the cell wall surface of R powder under the studied pH.

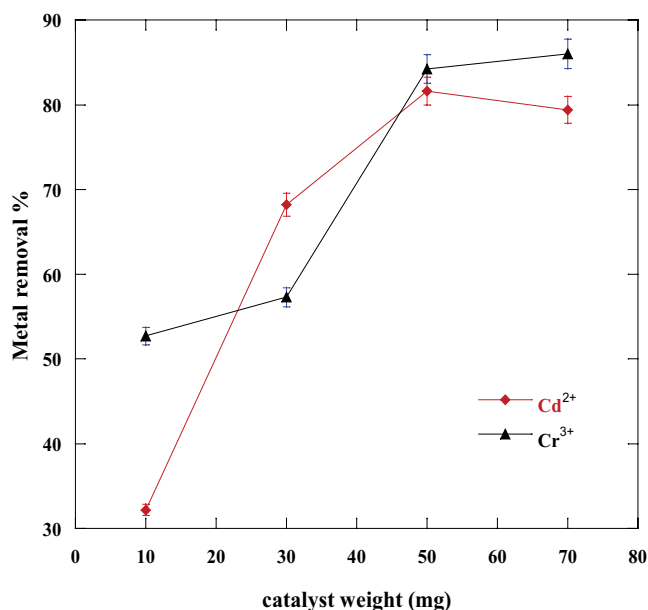


Fig. 7. Effect of catalyst weight on the removal % of Cd²⁺ and Cr³⁺ at 25°C and pH 6.2.

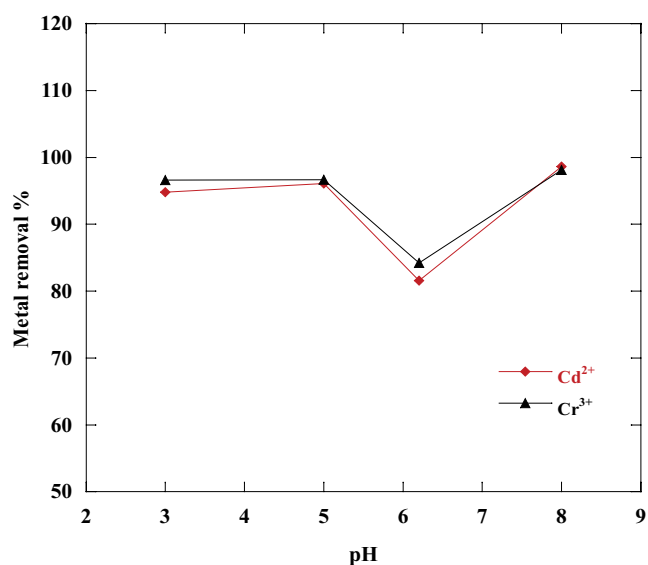


Fig. 8. Effect of pH on the removal of Cd²⁺ and Cr³⁺ by 50 mg of R at 25°C.

At pH 8, the removal percentage was very high. This may arise due to the predominant presence of hydrated species of heavy metals, precipitation of the appropriate salts and changes on the catalyst surface morphology [57].

3.7. Temperature effect

The adsorption of metal ions was done at 25°C, 40°C, 60°C, and 80°C using R as an adsorbent. The practical results showed that the adsorption capacity of Cr³⁺ onto R decreased with an increase in the temperature of the solution (Fig. 9). This implies that the adsorption of Cr³⁺ on the adsorbent R

is an exothermic process [58]. This decrease in biosorption capacity between 25°C and 80°C for Cr³⁺ can be attributed to the damage of active sites in the *R* waste. Many other researchers have also observed the same results [21,59]. For Cd²⁺ metal, there is slight effect of temperature on the removal % with increasing temperature from 25°C and 80°C where the adsorption capacity increases as the solution temperature increases in the range 25°C–40°C which indicates that cadmium adsorption is an endothermic process as reported in literature [60], then increasing the temperature over 40°C causes damage in active sites consequently the adsorption capacity decreases.

3.8. Reusability of *R*

The suitability of *R* to be used numerous times in the removal of Cd²⁺ and Cr³⁺ from wastewater was investigated

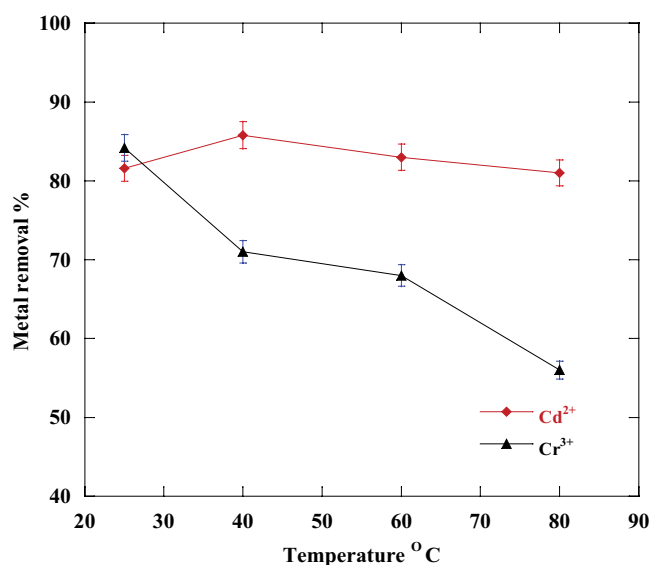


Fig. 9. Effect of temperature on the removal of Cd²⁺ and Cr³⁺ by 50 mg of *R* at pH 6.2.

and is shown in Fig. 10. The operating conditions were adjusted at 50 mg adsorbent mass, 100 mg L⁻¹ initial concentrations for the studied metal ions, 100 mL solution volume, 180 min reaction time and pH 6.2. After each run, the solid was collected after filtration and washed several times by distilled water to be used in the second run. The material showed high stability for the studied four runs and achieved high removal percentages for all the studied metal pollutants with a noticeable decrease in the efficiency from cycle 1 to cycle 4. The estimated removal percentages for Cd²⁺ ions are 81.8%, 75.8%, 75.5%, and 74.9% for cycle 1, cycle 2, cycle 3, and cycle 4, respectively. The recorded removal percentages for chromium ions were decreased to 84.7%, 80%, 76.4%, and 61.6% with repeating the removal cycles from cycle 1 to cycle 4 in order. This reduction can be attributed to the

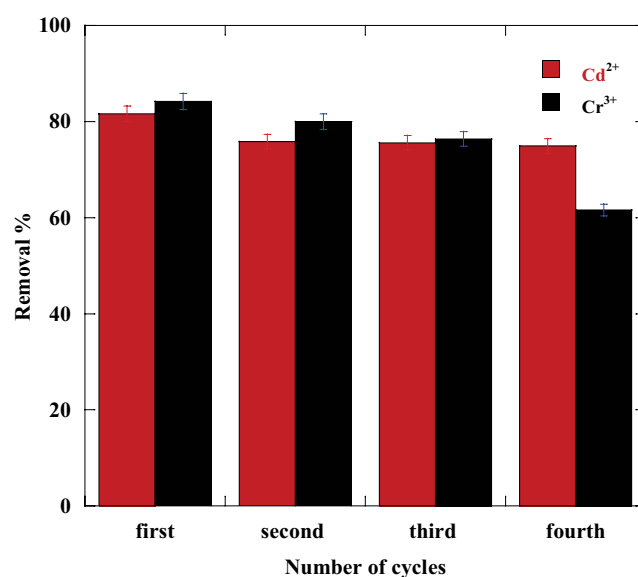


Fig. 10. Reusability of *R* for removal of Cd²⁺ and Cr³⁺ by 50 mg of *R* at 25°C and pH 6.2.

Table 3
Adsorption capacity of different adsorbents for Cd²⁺ and Cr³⁺ adsorption

Adsorbent	Cd ²⁺		Adsorbent	Cr ³⁺	
	Adsorption capacity q_m (mg g ⁻¹)	Reference		Adsorption capacity q_m (mg g ⁻¹)	Reference
Activated carbon	10.3	[13]	Borax sludge	16	[15]
Activated carbon	2.8	[28]	Modified lignin	25	[65]
MWCNTs	4.5	[28]	Carrot residues	45.09	[66]
Orange peel-Fe ₂ O ₃	71.43	[67]	<i>Spirogyra</i> spp.	30.21	[68]
Coffee grounds	15.65	[69]	Untreated <i>Pinus sylvestris</i> bark	8.69	[70]
Bamboo charcoal	12.08	[71]	Treated <i>Pinus sylvestris</i> bark	9.77	[70]
<i>Jatropha curcas</i> husk	8.35	[72]	<i>Pinus pinaster</i> bark	19.45	[73]
Commercial activated carbon	14.93	[72]	Sphagnum moss peat	29	[74]
<i>R</i>	81.76	This work	<i>R</i>	31.5	This work

deposition of metal ion particles on the surface of *R*, which results in blockage of adsorbent pores and finally in decrease in adsorption capacity [61] and this was confirmed from SEM images (Figs. 2(c) and (d)).

The results of the present work show that the generation of *R* to be re-used decreases from cycle 1 to cycle 4 in agreement with previous studies [61–64].

These results also show that *R* is an excellent reusable adsorbent for the removal of both Cd²⁺ and Cr³⁺ ions from the aqueous environment.

3.9. Comparison of adsorption capability of *R* with other adsorbents

The adsorption capacities (q_m) of different adsorbents for adsorption of Cd²⁺ and Cr³⁺ ions reported in the literature are compared in Table 3. It may be seen that q_m values differ widely for different adsorbents [13,15,28,65–74].

Comparison of q_m values shows that *R* exhibits a reasonable capacity for Cd²⁺ and Cr³⁺ adsorption from aqueous solutions.

4. Conclusions

In this study, we focused on the adsorption of Cd²⁺ and Cr³⁺ ions onto *R* from aqueous solutions. The results showed that *R* as waste material could be used as an efficient adsorbent for Cd²⁺ and Cr³⁺ metal ions where the highest removal percentages, are 98.6% and 98.1% for Cd²⁺ and Cr³⁺, respectively, at pH 8, 50 mg of catalyst, 25°C and initial metal concentration of 100 mg L⁻¹. Different adsorption models (Langmuir, Freundlich, and Temkin) were studied to describe the adsorption of cadmium and chromium onto *R*. It was found that the adsorption of Cd²⁺ fitted with Freundlich isotherm but Cr³⁺ was compatible with Temkin model. Also adsorption kinetics, the pseudo-first-order, pseudo-second-order, intraparticle diffusion, and simple Elovich kinetic models, were studied for both metal ions to determine the rate and mechanism of adsorption where it was found that the adsorption process followed the pseudo-second-order adsorption mechanism, which indicates that the adsorption mechanism is occurring chemically. This was elucidated by the data obtained from FTIR, which shows the presence of functional groups which have the ability to make chemical bonds with heavy metals and the maximum amounts of metals ions adsorbed were found to be 81.76 and 31.5 mg g⁻¹ for Cd²⁺ and Cr³⁺, respectively. Finally, it was concluded that *Rumex dentatus* waste was an effective low-cost adsorbent which was a reusable and eco-friendly biosorbent for Cd²⁺ and Cr³⁺ ions from aqueous solutions.

Acknowledgment

We acknowledge Dr. Gamal Abdel Maksoud, professor of English language at Nahda University, Beni-suef, Egypt, for his help and advices.

References

- [1] S. Franca, C. Vinagre, I. Cacador, H.N. Cabral, Heavy metal concentrations in sediment, benthic invertebrates and fish in three salt marsh areas subjected to different pollution loads in the Tagus Estuary (Portugal), *Mar. Pollut. Bull.*, 50 (2005) 998–1003.
- [2] W.H.O., UNICEF, WSSCC, Global Water Supply and Sanitation Assessment 2000 Report, 2000.
- [3] M.A. Zaini, R. Okayama, M. Machida, Adsorption of aqueous metal ions on cattle-manure-compost based activated carbons, *J. Hazard. Mater.*, 170 (2009) 1119–1124.
- [4] T.A. Davis, B. Volesky, R.H.S.F. Vieira, Sargassum seaweed as biosorbent for heavy metals, *Water Res.*, 34 (2000) 4270–4278.
- [5] S. Wilbur, H. Abadin, M. Fay, D. Yu, B. Tencza, L. Ingerman, J. Klotzbach, S. James, Toxicological Profile for Chromium, Agency for Toxic Substances and Disease Registry (US), Atlanta (GA), 2012.
- [6] C. Mant, S. Costa, J. Williams, E. Tambourgi, Studies of removal of chromium by model constructed wetland, *Braz. J. Chem. Eng.*, 22 (2005) 381–387.
- [7] M. Jaishankar, T. Tseten, N. Anbalagan, B.B. Mathew, K.N. Beeregowda, Toxicity, mechanism and health effects of some heavy metals, *Interdiscip. Toxicol.*, 7 (2014) 60–72.
- [8] WHO, Guidelines for drinking water quality, World Health Organization, Geneva, 2008.
- [9] M. John, S. Heuss-Assbichler, A. Ullrich, D. Rettenwander, Purification of heavy metal loaded wastewater from electroplating industry under synthesis of delafossite (ABO₂) by "Lt-delafossite process", *Water Res.*, 100 (2016) 98–104.
- [10] I.H. Chowdhury, M.K. Naskar, Hexagonal sheet-like mesoporous titanium phosphate for highly efficient removal of lead ion from water, *RSC Adv.*, 6 (2016) 67136–67142.
- [11] T. Viraraghavan, M. Dronamraju, Removal of copper, nickel and zinc from wastewater by adsorption using feat, *J. Environ. Sci. Health Part A*, 28 (1993) 1261–1276.
- [12] O.E. Abdel Salam, N.A. Reiad, M.M. ElShafei, A study of the removal characteristics of heavy metals from wastewater by low-cost adsorbents, *J. Adv. Res.*, 2 (2011) 297–303.
- [13] H. Shariffard, M. Nabavinia, M. Soleimani, Evaluation of adsorption efficiency of activated carbon/chitosan composite for removal of Cr (VI) and Cd (II) from single and bi-solute dilute solution, *Adv. Environ. Biol.*, 4 (2017) 215–227.
- [14] A.E. Burakov, E.V. Galunin, I.V. Burakova, A.E. Kucherova, S. Agarwal, A.G. Tkachev, V.K. Gupta, Adsorption of heavy metals on conventional and nanostructured materials for wastewater treatment purposes: a review, *Ecotoxicol. Environ. Saf.*, 148 (2018) 702–712.
- [15] F.T. Senberber, M. Yildirim, N.K. Mermer, E.M. Derun, Adsorption of Cr (III) from aqueous solution using borax sludge, *Acta Chim. Slov.*, 64 (2017) 654–660.
- [16] M.A. Elfotouh, K.A. Shams, K.P. Anthony, A.A. Shahat, M.T. Ibrahim, N.M. Abdelhady, N.S. Azim, F.M. Hammouda, M.M. El-Missiry, M.A. Saleh, Lipophilic Constituents of *Rumex vesicarius* L. and *Rumex dentatus* L., *Antioxidants (Basel)*, 2 (2013) 167–180.
- [17] A.A. Romeh, Efficiency of *Rumex dentatus* L. leaves extract for enhancing phytoremediation of *Plantago major* L. in soil contaminated by carbosulfan, *Soil Sediment Contam. Int. J.*, 25 (2016) 941–956.
- [18] M. Shaban, M.R. Abukhadra, M. Shahien, S.S. Ibrahim, Novel bentonite/zeolite-NaP composite efficiently removes methylene blue and Congo red dyes, *Environ. Chem. Lett.*, 16 (2018) 275–280.
- [19] M. Khedr, K.A. Halim, N. Soliman, Synthesis and photocatalytic activity of nano-sized iron oxides, *Mater. Lett.*, 63 (2009) 598–601.
- [20] X. Liu, W. Hu, X. Huang, H. Deng, Highly effective biosorption of Sr(II) from low level radioactive wastewater, *Water Sci. Technol.*, 71 (2015) 1727–1733.
- [21] A. Gundogdu, D. Ozdes, C. Duran, V.N. Bulut, M. Soyлак, H.B. Senturk, Biosorption of Pb(II) ions from aqueous solution by pine bark (*Pinus brutia* Ten.), *Chem. Eng. J.*, 153 (2009) 62–69.
- [22] M.M. Ghoneim, H.S. El-Desoky, K.M. El-Moselhy, A. Amer, E.H. Abou El-Naga, L.I. Mohamedein, A.E. Al-Prol, Removal of cadmium from aqueous solution using marine green algae, *Ulva lactuca*, *Egyptian J. Aquat. Res.*, 40 (2014) 235–242.
- [23] M.I. Shariful, T. Sepehr, M. Mehrali, B.C. Ang, M.A. Amalina, Adsorption capability of heavy metals by chitosan/poly(ethylene

- oxide)/activated carbon electrospun nanofibrous membrane, *J. Appl. Polym. Sci.*, 135 (2018) 45851.
- [24] B.Y.M. Bueno, M.L. Torem, F. Molina, L.M.S. de Mesquita, Biosorption of lead(II), chromium(III) and copper(II) by *R. opacus*: equilibrium and kinetic studies, *Miner. Eng.*, 21 (2008) 65–75.
- [25] K. Chhouk, W. Wahyudiono, H. Kanda, M. Goto, Comparison of conventional and ultrasound assisted supercritical carbon dioxide extraction of curcumin from turmeric (*Curcuma longa* L.), *Eng. J.*, 21 (2017) 53–65.
- [26] A. Saravanan, V. Brindha, S. Krishnan, Studies on the structural changes of the biomass *Sargassum* sp. on metal adsorption, *J. Adv. Bioinf.*, 2 (2011) 193–196.
- [27] N.M. Mahmoodi, Z. Mokhtari-Shourijeh, Modified poly (vinyl alcohol)-triethylenetetramine nanofiber by glutaraldehyde: preparation and dye removal ability from wastewater, *Desal. Wat. Treat.*, 57 (2016) 20076–20083.
- [28] A. Naghizadeh, Comparison between activated carbon and multiwall carbon nanotubes in the removal of cadmium (II) and chromium (VI) from water solutions, *J. Water Supply Res. Technol.*, 64 (2015) 64–73.
- [29] Y.C. Sharma, Optimization of parameters for adsorption of methylene blue on a low-cost activated carbon, *J. Chem. Eng. Data*, 55 (2009) 435–439.
- [30] I. Langmuir, The adsorption of gases on plane surfaces of glass, mica and platinum, *J. Am. Chem. Soc.*, 40 (1918) 1361–1403.
- [31] H. Freundlich, Over the adsorption in solution, *J. Phys. Chem.*, 57 (1906) 1100–1107.
- [32] K. Foo, B.H. Hameed, Insights into the modeling of adsorption isotherm systems, *Chem. Eng. J.*, 156 (2010) 2–10.
- [33] M. Temkin, V. Pyzhev, Kinetics of ammonia synthesis on promoted iron catalysts, *Acta physiochim. URSS*, 12 (1940) 217–222.
- [34] S. Bagherifam, S. Komarneni, A. Lakzian, A. Fotovat, R. Khorasani, W. Huang, J. Ma, S. Hong, F.S. Cannon, Y. Wang, Highly selective removal of nitrate and perchlorate by organoclay, *Appl. Clay Sci.*, 95 (2014) 126–132.
- [35] L. Sellaoui, H. Guedidi, S. Knani, L. Reinert, L. Duclaux, A.B. Lamine, Application of statistical physics formalism to the modeling of adsorption isotherms of ibuprofen on activated carbon, *Fluid Phase Equilib.*, 387 (2015) 103–110.
- [36] N.M. Mahmoodi, Synthesis of core-shell magnetic adsorbent nanoparticle and selectivity analysis for binary system dye removal, *J. Ind. Eng. Chem.*, 20 (2014) 2050–2058.
- [37] N.M. Mahmoodi, Synthesis of amine-functionalized magnetic ferrite nanoparticle and its dye removal ability, *J. Environ. Eng.*, 139 (2013) 1382–1390.
- [38] N.M. Mahmoodi, Dendrimer functionalized nanoarchitecture: synthesis and binary system dye removal, *J. Taiwan Inst. Chem. Eng.*, 45 (2014) 2008–2020.
- [39] N. Xin, X. Gu, H. Wu, Y. Hu, Z. Yang, Application of genetic algorithm-support vector regression (GA-SVR) for quantitative analysis of herbal medicines, *J. Chemometr.*, 26 (2012) 353–360.
- [40] N.M. Mahmoodi, B. Hayati, M. Arami, Kinetic, equilibrium and thermodynamic studies of ternary system dye removal using a biopolymer, *Ind. Crop Prod.*, 35 (2012) 295–301.
- [41] L. Fan, C. Luo, M. Sun, H. Qiu, X. Li, Synthesis of magnetic β -cyclodextrin-chitosan/graphene oxide as nanoadsorbent and its application in dye adsorption and removal, *Colloid Surf., B*, 103 (2013) 601–607.
- [42] H. Demiral, G. Gündüzoğlu, Removal of nitrate from aqueous solutions by activated carbon prepared from sugar beet bagasse, *Bioresour. Technol.*, 101 (2010) 1675–1680.
- [43] F.-C. Wu, R.-L. Tseng, R.-S. Juang, Characteristics of Elovich equation used for the analysis of adsorption kinetics in dye-chitosan systems, *Chem. Eng. J.*, 150 (2009) 366–373.
- [44] F.-C. Wu, R.-L. Tseng, R.-S. Juang, Initial behavior of intraparticle diffusion model used in the description of adsorption kinetics, *Chem. Eng. J.*, 153 (2009) 1–8.
- [45] A. Naghizadeh, F. Ghasemi, E. Derakhshani, H. Shahabi, Thermodynamic, kinetic and isotherm studies of sulfate removal from aqueous solutions by graphene and graphite nanoparticles, *Desal. Wat. Treat.*, 80 (2017) 247–254.
- [46] A. Naghizadeh, M. Ghafouri, A. Jafari, Investigation of equilibrium, kinetics and thermodynamics of extracted chitin from shrimp shell in reactive blue 29 (RB-29) removal from aqueous solutions, *Desal. Wat. Treat.*, 70 (2017) 355–363.
- [47] Z. Hu, H. Chen, F. Ji, S. Yuan, Removal of Congo Red from aqueous solution by cattail root, *J. Hazard. Mater.*, 173 (2010) 292–297.
- [48] H.A. Chanzu, J.M. Onyari, P.M. Shiundu, Biosorption of malachite green from aqueous solutions onto polylactide/spent brewery grains films: kinetic and equilibrium studies, *J. Polym. Environ.*, 20 (2012) 665–672.
- [49] B. Hameed, Evaluation of papaya seeds as a novel non-conventional low-cost adsorbent for removal of methylene blue, *J. Hazard. Mater.*, 162 (2009) 939–944.
- [50] M.P. Pons, M.C. Fuste, Uranium uptake by immobilized cells of *Pseudomonas* strain EPS 5028, *Appl. Microbiol. Biotechnol.*, 39 (1993) 661–665.
- [51] A. Esposito, F. Pagnanelli, A. Lodi, C. Solisio, F. Veglio, Biosorption of heavy metals by *Sphaerotilus natans*: an equilibrium study at different pH and biomass concentrations, *Hydrometallurgy*, 60 (2001) 129–141.
- [52] A. El-Sikaily, A. El Nemr, A. Khaled, Copper sorption onto dried red alga *Pterocladia capillacea* and its activated carbon, *Chem. Eng. J.*, 168 (2011) 707–714.
- [53] S.V. Mohan, N.C. Rao, J. Karthikeyan, Adsorptive removal of direct azo dye from aqueous phase onto coal based sorbents: a kinetic and mechanistic study, *J. Hazard. Mater.*, 90 (2002) 189–204.
- [54] K. Foo, B. Hameed, Preparation, characterization and evaluation of adsorptive properties of orange peel based activated carbon via microwave induced K_2CO_3 activation, *Bioresour. Technol.*, 104 (2012) 679–686.
- [55] M. Sprynsky, B. Buszewski, A.P. Terzyk, J. Namieśnik, Study of the selection mechanism of heavy metal (Pb^{2+} , Cu^{2+} , Ni^{2+} , and Cd^{2+}) adsorption on clinoptilolite, *J. Colloid Interface Sci.*, 304 (2006) 21–28.
- [56] Q. Li, J. Zhai, W. Zhang, M. Wang, J. Zhou, Kinetic studies of adsorption of Pb(II), Cr(III) and Cu(II) from aqueous solution by sawdust and modified peanut husk, *J. Hazard. Mater.*, 141 (2007) 163–167.
- [57] I. Kula, M. Uğurlu, H. Karaoğlu, A. Celik, Adsorption of Cd (II) ions from aqueous solutions using activated carbon prepared from olive stone by $ZnCl_2$ activation, *Bioresour. Technol.*, 99 (2008) 492–501.
- [58] A. Rahmani, H.Z. Mousavi, M. Fazli, Effect of nanostructure alumina on adsorption of heavy metals, *Desalination*, 253 (2010) 94–100.
- [59] S.N. Farhan, A.A. Khadom, Biosorption of heavy metals from aqueous solutions by *Saccharomyces cerevisiae*, *Int. J. Ind. Chem.*, 6 (2015) 119–130.
- [60] K.S. Rao, S. Anand, P. Venkateswarlu, Cadmium removal from aqueous solutions using biosorbent *Syzygium cumini* leaf powder: kinetic and equilibrium studies, *Korean J. Chem. Eng.*, 27 (2010) 1547–1554.
- [61] A. Naghizadeh, Regeneration of carbon nanotubes exhausted with humic acid using electro-Fenton technology, *Arab. J. Sci. Eng.*, 41 (2016) 155–161.
- [62] A. Naghizadeh, F. Momeni, E. Derakhshani, Efficiency of ultrasonic process in regeneration of graphene nanoparticles saturated with humic acid, *Desal. Wat. Treat.*, 70 (2017) 290–293.
- [63] E. Derakhshani, A. Naghizadeh, Ultrasound regeneration of multi wall carbon nanotubes saturated by humic acid, *Desal. Wat. Treat.*, 52 (2014) 7468–7472.
- [64] A. Naghizadeh, S. Nasser, A.H. Mahvi, A. Rashidi, R. Nabizadeh, R.R. Kalantary, Fenton regeneration of humic acid-spent carbon nanotubes, *Desal. Wat. Treat.*, 54 (2015) 2490–2495.
- [65] A. Demirbaş, Adsorption of Cr (III) and Cr (VI) ions from aqueous solutions on to modified lignin, *Energy Sources*, 27 (2005) 1449–1455.
- [66] B. Nasernejad, T.E. Zadeh, B.B. Pour, M.E. Bygi, A. Zamani, Comparison for biosorption modeling of heavy metals (Cr (III), Cu (II), Zn (II)) adsorption from wastewater by carrot residues, *Process Biochem.*, 40 (2005) 1319–1322.

- [67] V. Gupta, A. Nayak, Cadmium removal and recovery from aqueous solutions by novel adsorbents prepared from orange peel and Fe_2O_3 nanoparticles, *Chem. Eng. J.*, 180 (2012) 81–90.
- [68] N.R. Bishnoi, R. Kumar, S. Kumar, S. Rani, Biosorption of Cr (III) from aqueous solution using algal biomass *spirogyra* spp., *J. Hazard. Mater.*, 145 (2007) 142–147.
- [69] N. Azouaou, Z. Sadaoui, A. Djaafri, H. Mokaddem, Adsorption of cadmium from aqueous solution onto untreated coffee grounds: equilibrium, kinetics and thermodynamics, *J. Hazard. Mater.*, 184 (2010) 126–134.
- [70] M.M. Alves, C.G. Beca, R.G. De Carvalho, J. Castanheira, M.S. Pereira, L. Vasconcelos, Chromium removal in tannery wastewaters “polishing” by *Pinus sylvestris* bark, *Water Res.*, 27 (1993) 1333–1338.
- [71] F.Y. Wang, H. Wang, J.W. Ma, Adsorption of cadmium (II) ions from aqueous solution by a new low-cost adsorbent—Bamboo charcoal, *J. Hazard. Mater.*, 177 (2010) 300–306.
- [72] F. Okeola, E. Odebunmi, F. Nwosu, T. Abu, A. Mohammed, A. Samuel, Removal of lead and cadmium ions from aqueous solution by adsorption onto *Jatropha curcas* activated carbon, *Nig. J. Pure Appl. Sci.*, 30 (2017) 2955–2964.
- [73] T. de Vasconcelos, Adsorption equilibria between pine bark and several ions in aqueous solution, 1. Cd (II), Cr (III) and H^+ , *Eur. Water Manage.*, 3 (1993) 29–39.
- [74] J. McLellan, C. Rock, Pretreating landfill leachate with peat to remove metals, *Water Air Soil Pollut.*, 37 (1988) 203–215.